PROCEEDINGS OF SCIENCE

$\Upsilon(nS)$ decays and spectroscopy at Belle

P. Krokovny* **(for the Belle Collaboration)**
Budker Institute of Nuclear Physics SB RAS and Novosibirsk State University
E-mail: krokovny@inp.nsk.su

We search for bottomonium states in $\Upsilon(2S) \to (b\bar{b})\gamma$ decays using 158×10^6 $\Upsilon(2S)$ events collected with the Belle detector at the KEKB e^+e^- collider. The $(b\bar{b})$ system is reconstructed in 26 exclusive hadronic final states composed of charged pions, kaons, protons, and K^0_S mesons. We find no evidence for the state recently observed around 9975 MeV ($X_{b\bar{b}}$) in an analysis based on a data sample of 9.3×10^6 $\Upsilon(2S)$ events collected with the CLEO III detector. We set a 90% confidence level upper limit on the branching fraction $\mathscr{B}[\Upsilon(2S) \to X_{b\bar{b}}\gamma] \times \sum_i \mathscr{B}[X_{b\bar{b}} \to h_i] < 4.9 \times 10^{-6}$. This result is an order of magnitude smaller than the measurement reported with CLEO data. We also set an upper limit for the $\eta_b(1S)$ state of $\mathscr{B}[\Upsilon(2S) \to \eta_b(1S)\gamma] \times \sum_i \mathscr{B}[\eta_b(1S) \to h_b(iP)] < 3.7 \times 10^{-6}$. We also report the results of a high-statistics search for H-dibaryon production in inclusive $\Upsilon(1S)$ and $\Upsilon(2S)$ decays based on analyses of 102×10^6 $\Upsilon(1S)$ and 158×10^6 $\Upsilon(2S)$ events collected with the Belle detector at the KEKB e^+e^- collider. No indication of an H-dibaryon with mass near the $M_H = 2m_\Lambda$ threshold is seen in either the $H \to \Lambda p\pi^-$ or $\Lambda\Lambda$ decay channels and 90% confidence level branching-fraction upper limits are set that are between one and two orders of magnitude below the measured branching fractions for inclusive $\Upsilon(1S)$ and $\Upsilon(2S)$ decays to antideuterons. Since $\Upsilon(1,2S)$ decays produce flavor-$SU(3)$-symmetric final states, these results put stringent constraints on H-dibaryon properties.

The European Physical Society Conference on High Energy Physics
18-24 July, 2013
Stockholm, Sweden

*Speaker.

PoS(EPS-HEP 2013)357

1. Introduction

Bottomonium is the bound system of $b\bar{b}$ quarks and is considered an excellent laboratory to study Quantum Chromodynamics (QCD) at low energies. The system is approximately non-relativistic due to the large b quark mass, and therefore the quark-antiquark QCD potential can be investigated via $b\bar{b}$ spectroscopy.

We use data samples containing 102 million $\Upsilon(1S)$ and 158 million $\Upsilon(2S)$ decays collected with the Belle detector [1] operating at the KEKB e^+e^- collider [2]. The data were accumulated at center-of-mass system (cms) energies of $\sqrt{s} = 9.460$ GeV and 10.023 GeV, which correspond to the $\Upsilon(1S)$ and $\Upsilon(2S)$ resonance peaks, respectively.

2. Search for Bottomonium States in Exclusive Radiative $\Upsilon(2S)$ Decays

We report a search for the states $X_{b\bar{b}}$ in $\Upsilon(2S) \to X_{b\bar{b}}\gamma$ decays and $\eta_b(1S)$ in $\Upsilon(2S) \to \eta_b(1S)\gamma$ decays. This analisys is decribed in more details in Ref. [4]. We reconstruct $(b\bar{b})$ system in 26 modes reported in Ref. [3]. We require all charged tracks, except for those from K^0_S decays, to originate from the vicinity of the interaction point (IP). Track candidates are identified as pions, kaons, or protons based on information from the CDC, the TOF and the ACC. Candidate K^0_S mesons are reconstructed by combining two oppositely charged tracks (with a pion mass assumed for both) with an invariant mass between 486 and 509 MeV/c^2; the selected candidates are also required to have decay vertex displaced from the IP. We then combine a photon candidate with the $(b\bar{b})$ system to form an $\Upsilon(2S)$ candidate. The photon is reconstructed from an isolated (not matched to any charged track) cluster in the ECL that has an energy greater than 22 MeV and a cluster shape consistent with an electromagnetic shower. The energy of the signal photon is $30-70$ MeV and $400-900$ MeV for the $X_{b\bar{b}}$ and $\eta_b(1S)$, respectively. We exclude photons from the backward endcap in the $\eta_b(1S)$ selection to suppress low-energy photons arising from beam-related background. For the $X_{b\bar{b}}$ selection, both the backward and forward endcap regions are excluded. The signal windows for the difference between the energy of the $\Upsilon(2S)$ candidate and the CM energy (ΔE) and the $\Upsilon(2S)$ momentum measured in the CM frame ($P^*_{\Upsilon(2S)}$) are optimized separately for the $X_{b\bar{b}}$ and $\eta_b(1S)$ mass regions. We perform this optimization using a figure-of-merit $S/\sqrt{S+B}$, where S is the expected signal based on MC simulations, and B is the background estimated from a sum of the $\Upsilon(4S)$ off-resonance data, scaled to the available $\Upsilon(2S)$ integrated luminosity, and the inclusive $\Upsilon(2S)$ MC sample described earlier. The value of S is calculated by assuming the branching fraction to be 46.2×10^{-6} for the $X_{b\bar{b}}$ [3] and 3.9×10^{-6} for the $\eta_b(1S)$ [5]. The $\Upsilon(2S)$ candidates with $-40\,\text{MeV} < \Delta E < 50\,\text{MeV}$ and $P^*_{\Upsilon(2S)} < 30\,\text{MeV}/c$ [$-30\,\text{MeV} < \Delta E < 80\,\text{MeV}$ and $P^*_{\Upsilon(2S)} < 50\,\text{MeV}/c$] are retained for a further study of the $X_{b\bar{b}}$ [$\eta_b(1S)$] state. For the two-body decay hypothesis, the angle $\theta_{(b\bar{b})\gamma}$ between the reconstructed $(b\bar{b})$ system and the photon candidate in the CM frame should be close to 180°. We apply an optimized requirement on $\theta_{(b\bar{b})\gamma}$ to be greater than 150° [177°] to select the $\Upsilon(2S) \to X_{b\bar{b}}\gamma$ [$\Upsilon(2S) \to \eta_b(1S)\gamma$] decay candidates. The difference between the invariant mass formed by combining the signal photon with another photon candidate in the event and the nominal π^0 mass [7] is computed for each photon pair; the smallest of the magnitudes of these differences is denoted by $\Delta M_{\gamma\gamma}$ and used for a π^0 veto. For the $\eta_b(1S)$ selection, where the background contribution is dominated by π^0's coming from the $\Upsilon(2S)$ decays,

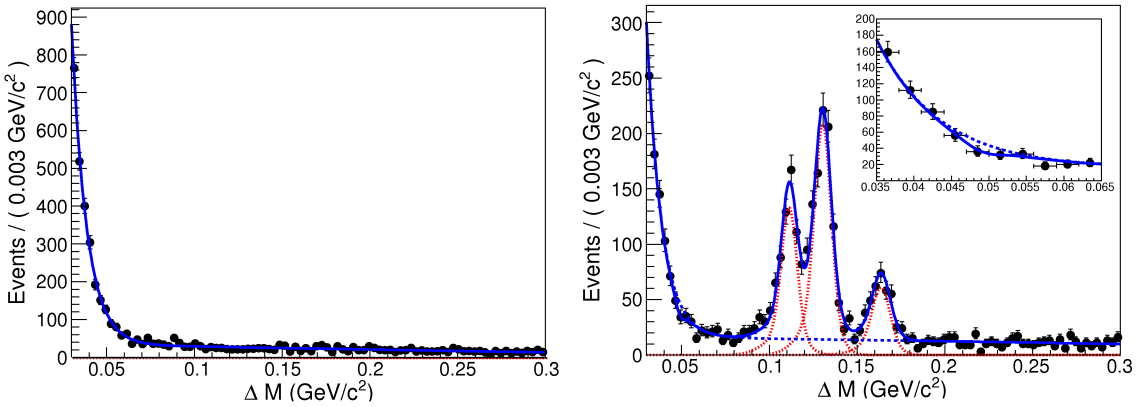

Figure 1: The ΔM distributions for (left) $\Upsilon(4S)$ off-resonance data and (right) $\Upsilon(2S)$ data events that pass the selection criteria. Points with error bars are the data, curves show the fit results. The right inset shows an expanded view of the ΔM distribution in the $[0.035, 0.065]\,\mathrm{GeV}/c^2$ region.

we require $\Delta M_{\gamma\gamma} > 10\,\mathrm{MeV}/c^2$. The final selection efficiencies for the individual modes range from 6.1% to 1.2%.

We apply a kinematic fit to the $\Upsilon(2S)$ candidates constrained by energy-momentum conservation. The resolution of the reconstructed invariant mass of the $\eta_b(1S)$, presented in terms of $\Delta M \equiv M[(b\bar{b})\gamma] - M(b\bar{b})$, is significantly improved by this fit from approximately 14 to $8\,\mathrm{MeV}/c^2$. The fit χ^2 value is used to select the best $\Upsilon(2S)$ candidate in the case of multiple candidates that appear in about 10% of the events satisfying the $X_{b\bar{b}}$ selection.

We extract the signal yield by performing an unbinned extended maximum-likelihood fit to the ΔM distribution for all selected candidates. The probability density functions (PDFs) for $\chi_{bJ}(1P)$ and $X_{b\bar{b}}$ signals are parametrized by the sum of a Gaussian and an asymmetric Gaussian function to take into account low-energy tails. Their parameters are taken from MC simulations. To account for the modest difference in the detector resolution between data and simulations, we use a calibration factor common to the four signal components, *i.e.*, $\chi_{bJ}(1P)$ with $J = 0, 1, 2$ and $X_{b\bar{b}}$, to smear their core Gaussian components. The choice of the background PDF is particularly important and is determined from the large sample of $\Upsilon(4S)$ off-resonance data. As shown in the top plot of Fig. 1, the best fit to these data is obtained by using a sum of an exponential function and a first-order Chebyshev polynomial for the $X_{b\bar{b}}$ region, whose parameters are allowed to vary in the fit. This is in contrast to Ref. [3], where a single exponential function was used to describe the background PDF. The polynomial component is needed to model the background due to final-state radiation for $\Delta M < 0.15\,\mathrm{GeV}/c^2$ and from π^0 for $\Delta M \geq 0.15\,\mathrm{GeV}/c^2$. We have verified using a large number of pseudoexperiments that if the $X_{b\bar{b}}$ signal is present in our data sample we would observe it with a significance above 10 standard deviations.

In the bottom plot of Fig. 1, we present fits to the ΔM distributions for the sum of the 26 modes in the $X_{b\bar{b}}$ region. The results of the fit show no evidence of an $X_{b\bar{b}}$ signal, with a yield of -30 ± 19 events. In the fits to the $\chi_{bJ}(1P)$ ($J = 0, 1, 2$) states we observe large signal yields and determine invariant masses of 9859.6 ± 0.5, 9892.8 ± 0.2 and $9912.0 \pm 0.3\,\mathrm{MeV}/c^2$, respectively, which are in excellent agreement with the corresponding world-average values [7]. The parameters

obtained for the background PDF in the $\Upsilon(2S)$ sample are consistent with those found in the fit to the $\Upsilon(4S)$ off-resonance data, giving us confidence in our background modeling. The signal PDF for the $\eta_b(1S)$ is a Breit-Wigner function, whose width is fixed to the value obtained in Ref. [6], convolved with a Gaussian function with a width of $8\,\mathrm{MeV}/c^2$ describing the detector resolution. A first-order Chebyshev polynomial is used for the background in the $\eta_b(1S)$ region, validated with the large sample of $\Upsilon(4S)$ off-resonance data. No signal (-6 ± 10 events) is found for the $\eta_b(1S)$.

The branching fraction is determined from the number of observed signal events ($n_{\rm sig}$) as $\mathscr{B} = n_{\rm sig}/\{\varepsilon[(b\bar{b})]\times N_{\Upsilon(2S)}\}$, where $\varepsilon[(b\bar{b})]$ is the average efficiency and $N_{\Upsilon(2S)}$ is the total number of $\Upsilon(2S)$ decays. In the absence of the signal, we obtain an upper limit at 90% confidence level (C.L.) on the branching fraction ($\mathscr{B}_{\rm UL}$) by integrating the likelihood ($\mathscr{L}$) of the fit with fixed values of the branching fraction: $\int_0^{\mathscr{B}_{\rm UL}}\mathscr{L}(\mathscr{B})d\mathscr{B} = 0.9\times\int_0^1\mathscr{L}(\mathscr{B})d\mathscr{B}$. Multiplicative systematic uncertainties are included by convolving the likelihood function with a Gaussian function with a width equal to the total uncertainty. We estimate $\mathscr{B}[\Upsilon(2S)\to\eta_b(1S)\gamma]\times\sum_i\mathscr{B}[\eta_b(1S)\to h_i] < 3.7\times10^{-6}$ and $\mathscr{B}[\Upsilon(2S)\to X_{b\bar{b}}\gamma]\times\sum_i\mathscr{B}[X_{b\bar{b}}\to h_i] < 4.9\times10^{-6}$.

3. Search for an H-dibaryon with mass near $2m_\Lambda$ in $\Upsilon(1S)$ and $\Upsilon(2S)$ decays

We search for H-dibaryon production in the inclusive processes $\Upsilon(1,2S)\to HX$; $H\to\Lambda p\pi^-$ and $\Lambda\Lambda$. This analisys is decribed in more details in Ref. [8]. We assume equal $\Upsilon(1S)$ and $\Upsilon(2S)$ branching fractions: *i.e.*, $\mathscr{B}(\Upsilon(1S)\to HX) = \mathscr{B}(\Upsilon(2S)\to HX)\equiv\mathscr{B}(\Upsilon(1,2S)\to HX)$. Λ candidates are reconstructed in $p\pi^-$ decay using the selection criteria described in Ref. [9]. We require $\Delta M_\Lambda\equiv|M(p\pi)-m_\Lambda| < 3.0$ MeV. For the $H\to\Lambda p\pi^-$ search, the $p\pi^-$ track selection requirements are optimized using *FoM*s determined by MC assuming $\tau_H=\tau_\Lambda$. Both the p and π^- are required to be well identified. We require that the p and π^- tracks and the Λ trajectory satisfy a fit to a common vertex with $\chi^2_{\Lambda p\pi^-}\le 50$. In addition we require $c\tau_{\Lambda p\pi^-}\ge 0.0$, where $c\tau\equiv\vec{\ell}\cdot\vec{p}_H M_H/|\vec{p}_H|^2$ and $\vec{\ell}$ is the displacement between the run-dependent average interaction point (IP) and the fitted vertex position. The $\Lambda\to p_1\pi_1^-$ candidate is subjected to a kinematic fit that constrains $M(p_1\pi_1^-)$ to m_Λ. The final selection efficiencies are determined from MC by averaging $\Upsilon(1S)$ & $\Upsilon(2S)$ signal MC to be $\varepsilon_1 = 7.7\%$ for $H\to\Lambda p\pi^-$ and $\bar{\varepsilon}_1 = 8.8\%$ for $\bar{H}\to\bar{\Lambda}\bar{p}\pi^+$. For the second Λ (Λ_2) in the $H\to\Lambda_1\Lambda_2$ ($\Lambda_i\to p_i\pi_i^-$) channel, in addition to the criteria used for Λ_1 selection, *FoM*s based on MC events are used to optimize the additional requirements $\chi^2_{\Lambda_1\Lambda_2} < 200$ from a $\Lambda_1\Lambda_2$ vertex and IP constrained fit, and $c\tau_{\Lambda_2}\ge -0.5$ cm. The $\Lambda\Lambda$ candidates are subjected to a kinematic fit that constrains both $p\pi^-$ masses to m_Λ. The MC-determined selection efficiencies, obtained by averaging $\Upsilon(1S)$ & $\Upsilon(2S)$ signal MC results, are $\varepsilon_2 = 10.9\%$ for $H\to\Lambda\Lambda$ and $\bar{\varepsilon}_2 = 10.1\%$ for $\bar{H}\to\bar{\Lambda}\bar{\Lambda}$.

The resulting continuum-subtracted $M(\Lambda p\pi^-)$ ($M(\bar{\Lambda}\bar{p}\pi^+)$) and $M(\Lambda\Lambda)$ ($M(\bar{\Lambda}\bar{\Lambda})$) distribution for the combined $\Upsilon(1S)$ and $\Upsilon(2S)$ samples, shown in the top (bottom) panel of Fig. 2, has no evident $H\to\Lambda p\pi^-$ ($\bar{H}\to\bar{\Lambda}\bar{p}\pi^+$) signal. There is no sign of a near-threshold enhancement similar to that reported by the E522 collaboration [10] nor any other evident signal for $H\to\Lambda\Lambda$ ($\bar{H}\to\bar{\Lambda}\bar{\Lambda}$). The curve in the figure is the result of a fit using an ARGUS-like threshold function to model the background fit residuals are also shown.

For each channel, we do a sequence of binned fits to the invariant mass distributions in Fig. 2 using a signal function to represent $H\to f_i$ ($f_1=\Lambda p\pi^-$ & $f_2=\Lambda\Lambda$) and an ARGUS function to represent the background. In the fits, the signal peak position is confined to a 4 MeV window that

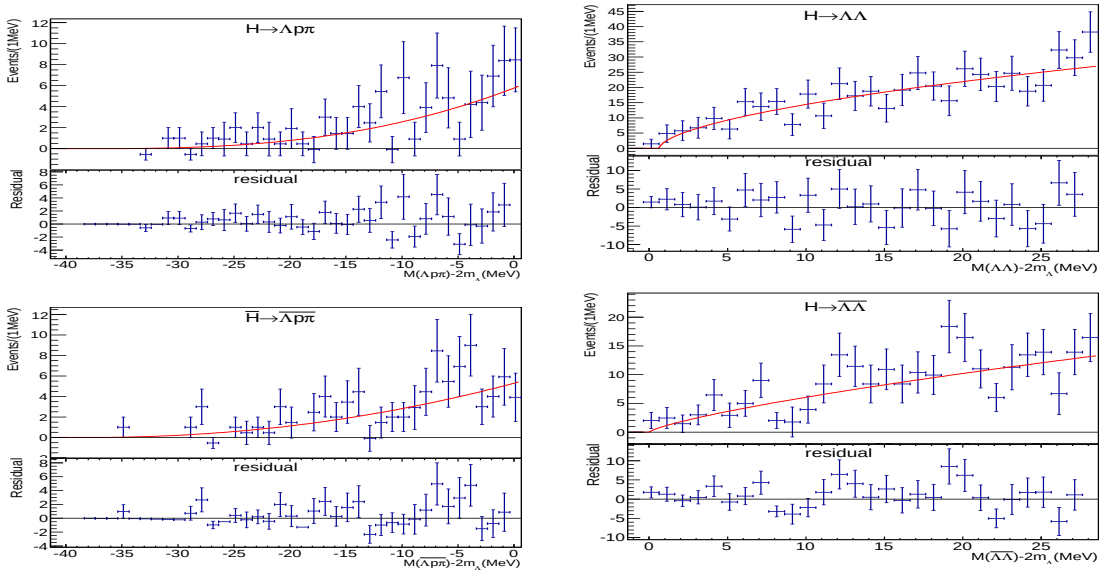

Figure 2: Top: the continuum-subtracted $M(\Lambda p\pi^-)$ distribution (left) and $M(\Lambda\Lambda)$ (right) for the combined $\Upsilon(1S)$ and $\Upsilon(2S)$ data samples. The curve shows the results of the background-only fit described in the text. Bottom: the corresponding $M(\bar{\Lambda}\bar{p}\pi^+)$ (left) and $M(\bar{\Lambda}\bar{\Lambda})$ (right) distributions.

is scanned in 4 MeV steps across the ranges $(m_\Lambda + m_p + m_{\pi^-}) \le M(\Lambda p\pi^-) \le 2m_\Lambda$ and $2m_\Lambda \le M(\Lambda\Lambda) \le 2m_\Lambda + 28$ MeV. For the $\Lambda p\pi^-$ ($\bar{\Lambda}\bar{p}\pi^+$) mode, the signal function is a Gaussian whose resolution width is fixed at its MC-determined value scaled by a factor $f = 0.85(1.12)$ that is determined from a comparison of data and MC fits to inclusive $\Xi^- \to \Lambda\pi^-$ and $\Xi_c^0(2470) \to \Xi^-\pi^+$ signals found in the same data samples. For the $\Lambda\Lambda$ mode, the signal function is a Lorentzian with FWHM fixed at either $\Gamma = 0$ or 10 MeV convolved with a Gaussian. Since the f_i and $\bar{f}_i$ acceptances are different, we fit the particle and antiparticle distributions separately.

None of the fits exhibit a positive signal with greater than 3σ significance. The fit results are translated into 90% CL upper limits on the signal yield, $N_i^{\rm UL}(M_H)$ and $\bar{N}_i^{UL}(M_H)$, by convolving the fit likelihood distribution with a Gaussian whose width equals the systematic error (discussed below) and then determining the yield below which 90% of the area above $N_i = 0$ is contained. These values are used to determine upper limits on the inclusive product branching fractions via the relation $\mathscr{B}(\Upsilon(1,2S) \to H\,X) \cdot \mathscr{B}(H \to f_i) < \frac{1}{2N_\Upsilon(\mathscr{B}_{\Lambda\to p\pi^-})^i} \frac{N_i^{\rm UL}(M_H)}{\varepsilon_i}$, where $N_\Upsilon = (260 \pm 6) \times 10^6$ is the total number of $\Upsilon(1S)$ plus $\Upsilon(2S)$ events in the data sample and $\mathscr{B}_{\Lambda\to p\pi^-} = 0.639 \pm 0.005$ [7].

For the final limits quoted in Table 1, we use the branching fraction value that contains $< 90\%$ of the above-zero area of the product of the H and $\bar{H}$ likelihood functions.

4. Conclusion

In summary, we have searched for the $X_{b\bar{b}}$ state reported in Ref. [3], that is reconstructed in 26 exclusive hadronic final states using a sample of $(157.8 \pm 3.6) \times 10^6$ $\Upsilon(2S)$ decays. We find no evidence for a signal and thus determine a 90% C.L. upper limit on the product branching fraction $\mathscr{B}[\Upsilon(2S) \to X_{b\bar{b}}\gamma] \times \sum_i \mathscr{B}[X_{b\bar{b}} \to h_i] < 4.9 \times 10^{-6}$, which is an order of magnitude smaller than the

Table 1: 90% CL upper limits ($\times 10^{-7}$) on the product branching fraction $\mathscr{B}(\Upsilon(1,2S) \to H\,X) \cdot \mathscr{B}(H \to f_i)$, $f_1 = \Lambda p\pi^-$; $\delta M_1 = 2m_\Lambda - M_H$ and $f_2 = \Lambda\Lambda$; $\delta M_2 = M_H - 2m_\Lambda$.

δM_i (MeV)	2	6	10	14	18	22	26	30	34
$f_1 = \Lambda p\pi^-$	15.	9.7	7.1	6.3	1.5	5.2	1.7	4.6	0.8
$f_2 = \Lambda\Lambda$, $\Gamma = 0$	6.0	9.6	2.2	11.	14.	9.2	2.5		
$\Gamma = 10$ MeV	16.	17.	15.	37.	44.	42.	33.		

branching fraction reported in Ref. [3]. We have also searched for the $\eta_b(1S)$ state and set an upper limit $\mathscr{B}[\Upsilon(2S) \to \eta_b(1S)\gamma] \times \sum_i \mathscr{B}[\eta_b(1S) \to h_i] < 3.7 \times 10^{-6}$ at 90% C.L.

We also report the most stringent constraints to date on the existence of an H-dibaryon with mass near the $2m_\Lambda$ threshold. These upper limits are between one and two orders of magnitude below the average of the PDG value for inclusive $\Upsilon(1S)$ and $\Upsilon(2S)$ decays to antideuterons. Since $\Upsilon \to$ hadrons decays produce final states that are flavor-$SU(3)$ symmetric, this suggests that if an H-dibaryon exists in this mass range, it must have very different dynamical properties than the deuteron, or, in the case of $M_H < 2m_\Lambda$, a strongly suppressed $H \to \Lambda p\pi^-$ decay mode.

We thank the KEKB group for excellent operation of the accelerator; the KEK cryogenics group for efficient solenoid operations; and the KEK computer group, the NII, and PNNL/EMSL for valuable computing and SINET4 network support. We acknowledge support from MEXT, JSPS and Nagoya's TLPRC (Japan); ARC and DIISR (Australia); NSFC (China); MSMT (Czechia); DST (India); INFN (Italy); MEST, NRF, GSDC of KISTI, and WCU (Korea); MNiSW (Poland); MES and RFAAE (Russia); ARRS (Slovenia); SNSF (Switzerland); NSC and MOE (Taiwan); and DOE and NSF (USA). This work is partially supported by grants of the Russian Foundation for Basic Research 12-02-01296, 12-02-01032, 12-02-31363 and 12-02-33015.

References

[1] A. Abashian *et al.* (Belle Collaboration), Nucl. Instrum. Methods Phys. Res., Sect. A **479**, 117 (2002); also see detector section in J.Brodzicka *et al.*, Prog. Theor. Exp. Phys. (2012) 04D001.

[2] S. Kurokawa and E. Kikutani, Nucl. Instrum. Methods Phys. Res. Sect. A **499**, 1 (2003), and other papers included in this Volume; T.Abe *et al.*, Prog. Theor. Exp. Phys. (2013) 03A001-03A011.

[3] S. Dobbs, Z. Metreveli, A. Tomaradze, T. Xiao and K.K. Seth, Phys. Rev. Lett. **109**, 082001 (2012).

[4] S. Sandilya, K. Trabelsi, G. Mohanty *et al.* (Belle Collaboration) Phys. Rev. Lett. **111**, 11201 (2013).

[5] B. Aubert *et al.* (BaBar Collaboration), Phys. Rev. Lett. **103**, 161801 (2009).

[6] R. Mizuk *et al.* (Belle Collaboration), Phys. Rev. Lett. **109**, 232002 (2012).

[7] J. Beringer et al. *et al.* (Particle Data Group), Phys. Rev. D **86**, 010001 (2012).

[8] B. H. Kim, S. Olsen, *et al.* (Belle collaboration), Phys. Rev. Lett. **110**, 222002 (2013).

[9] K. Abe *et al.* (Belle Collaboration), Phys. Rev. D **65**, 091103 (2002).

[10] C.J. Yoon *et al.*, (KEK-PS E522 Collaboration), Phys. Rev. C **75**, 022201(R) (2007). See also J.K. Ahn *et al.*, (KEK-PS E224 Collaboration), Phys. Lett. **B444**, 267 (1998) and J. Belz *et al.*, (BNL E888 Collaboration), Phys. Rev. D **53**, 3487 (1996).